

# Catalytic Hydrodefluorination via Oxidative Addition, Ligand Metathesis, and Reductive Elimination at Bi(I)/Bi(III) Centers

Yue Pang, Markus Leutzsch, Nils Nöthling, Felix Katzenburg, and Josep Cornella\*



Cite This: *J. Am. Chem. Soc.* 2021, 143, 12487–12493



Read Online

ACCESS |



Metrics & More



Article Recommendations



Supporting Information

**ABSTRACT:** Herein, we report a hydrodefluorination reaction of polyfluoroarenes catalyzed by bismuthinidenes, Phebox-Bi(I) and OMe-Phebox-Bi(I). Mechanistic studies on the elementary steps support a Bi(I)/Bi(III) redox cycle that comprises C(sp<sup>2</sup>)-F oxidative addition, F/H ligand metathesis, and C(sp<sup>2</sup>)-H reductive elimination. Isolation and characterization of a cationic Phebox-Bi(III)(4-tetrafluoropyridyl) triflate manifests the feasible oxidative addition of Phebox-Bi(I) into the C(sp<sup>2</sup>)-F bond. Spectroscopic evidence was provided for the formation of a transient Phebox-Bi(III)(4-tetrafluoropyridyl) hydride during catalysis, which decomposes at low temperature to afford the corresponding C(sp<sup>2</sup>)-H bond while regenerating the propagating Phebox-Bi(I). This protocol represents a distinct catalytic example where a main-group center performs three elementary organometallic steps in a low-valent redox manifold.

The elementary organometallic steps, oxidative addition (OA), ligand metathesis (LM), and reductive elimination (RE), define the innate capacity of transition-metal centers to revolve between different oxidation states in numerous catalytic processes (Figure 1A).<sup>1</sup> With the aim of mimicking such reactivity by elements beyond the d-block, the past decades have witnessed prominent progress in low-valent main-group compounds exhibiting transition-metal-like reactivity, in particular, the cleavage of strong chemical bonds (e.g., N-H, O-H, H-H, C-H, C-F) through OA.<sup>2</sup> However, the intrinsic difficulties posed by the regeneration of low-valent species via RE limited the development of efficient catalytic redox processes based on main-group catalysts.<sup>2b,c</sup> Located in the middle of the p-block, group 15 elements have recently been identified as privileged candidates to unfold redox catalysis,<sup>3</sup> as exemplified by the success of redox cycling using P and Bi redox couples in various catalytic reactions.<sup>4-6</sup> In this endeavor, our group reported catalytic C(sp<sup>2</sup>)-F and C(sp<sup>2</sup>)-OTf/ONf bond formation proceeding through canonical cross-coupling steps in a Bi(III)/Bi(V) manifold (Figure 1B).<sup>5</sup> However, in contrast to other pnictogens, Bi possesses additional low-valent redox manifolds to be exploited. Indeed, the Bi(I)/(III) redox couple has recently emerged and found applications in catalytic transfer hydrogenation of azo- and nitro-arenes, as well as in the catalytic activation of N<sub>2</sub>O.<sup>6</sup> The low-valent Bi(I)/(III) redox manifold distinguishes itself from the high-valent and radical processes<sup>7</sup> by its superior catalytic efficiency, and achieving catalytic redox transformations via the full triad of three elementary organometallic steps would be highly desirable.

Hydrodefluorination (HDF) of polyfluoroarenes is a fundamental reaction that enables access to partially fluorinated building blocks from perfluorinated bulk chemicals.<sup>8</sup> HDFs have largely been dominated by transition-metal catalysis,<sup>9,10</sup> and a considerable number of these systems proceed through the catalytic steps depicted in Figure 1A.<sup>10</sup>

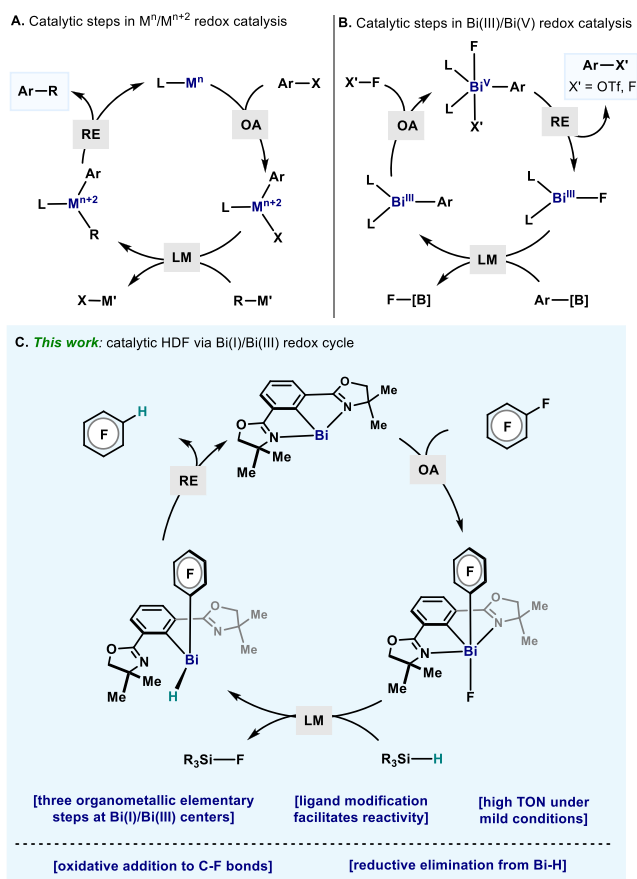
Recent progress in HDFs extended the available strategies to photoredox catalysis<sup>11</sup> and main-group catalysis,<sup>12,13</sup> which proceed through mechanistically distinct catalytic steps. In addition to its synthetic potential, HDF serves as a model reaction for studying the performance of main-group compounds in the elementary organometallic steps of a catalytic cycle. In this regard, C-F OA has been established for low-valent group 13/14 elements,<sup>14</sup> and recently Radosevich has further shown an elegant synthetic cycle for HDF at a phosphorus triamide.<sup>15</sup> Herein, we report that bismuthinidenes with a rationally designed *N,C,N*-pincer ligand scaffold unlock the catalytic HDF of a variety of polyfluoroarenes (Figure 1C). Mechanistic studies suggest a Bi(I)/Bi(III) cycle comprising C-F OA, F/H LM, and C-H RE steps, in a manner akin to a canonical catalytic cycle of transition-metal congeners.

Initially, we attempted the HDF of hexafluorobenzene (**1a**) using 5 mol% of Dostál's bismuthinidene **3**<sup>16</sup> as catalyst and 2.4 equiv. of Et<sub>2</sub>SiH<sub>2</sub> as hydrogen source in THF at 60 °C (Figure 2A). Unfortunately, only a trace amount of HDF product (**2a**, <1%) was detected after 20 h. With the aim of tuning the electronics of the Bi(I) center, an alternative *N,C,N*-pincer scaffold was envisaged, where the imine arms are replaced with oxazoline groups. In this manner, two new bismuthinidenes supported by a 2,6-bis(oxazolonyl)phenyl (Phebox) ligand scaffold,<sup>17</sup> Phebox-Bi(I) (**4**) and OMe-Phebox-Bi(I) (**5**), were synthesized via cobaltocene reduction of the parent bismuth chlorides **6** and **7**.<sup>6b,18</sup> When **4** and **5**

Received: June 29, 2021

Published: August 6, 2021

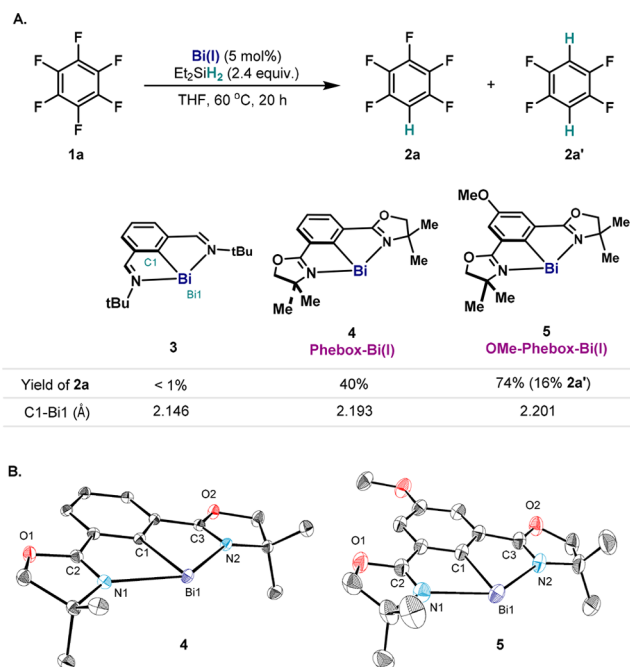




**Figure 1.** (A) Well-established transition-metal catalytic cycle. (B) Bi(III)/Bi(V) redox catalysis including elementary organometallic steps of OA/LM/RE. (C) HDF via Bi(I)/Bi(III) catalysis: elementary organometallic steps at low-valent main-group centers.

were tested as catalysts for the HDF of **1a**, 40% and 74% of **2a** were obtained, respectively. In the case of **5**, two-fold HDF (**2a'**) could also be detected in 16% yield. To gain more insights on the boosted reactivity, X-ray crystal structures of **4** and **5** were compared with that of **3**, showing considerably more elongated Bi1–C1 distances [2.193(6) Å for **4**,<sup>19</sup> 2.201(2) Å for **5**, cf. 2.146(18) Å for **3**,<sup>19</sup> Figure 2B]. These data suggest that electron delocalization of the  $6p_z^2$  lone pair of Bi to the *ipso* C( $sp^2$ ) is diminished in the new bismuthinidene, leading to the enhanced reactivity of the Phebox-based Bi(I) in HDFs.<sup>16,20</sup>

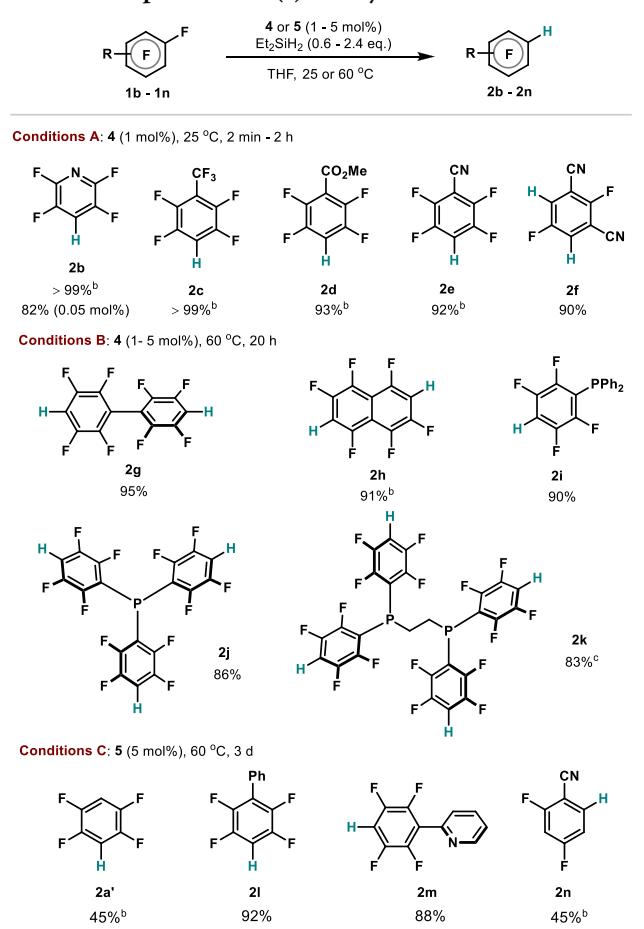
With these Bi(I) catalysts in hand, HDFs of other polyfluoroarenes were evaluated (**1b–1n**, Table 1). In general, HDF proceeds in high yields; however, the reaction parameters varied significantly depending on the substituents of the substrates.<sup>18</sup> Pentafluoropyridine (**1b**) and pentafluorobenzenes with strong electron-withdrawing groups ( $CF_3$ ,  $CO_2Me$ , and  $CN$ , **1c–1f**) underwent HDF readily at ambient temperature. Whereas **1b** reached full conversion in 1 h using **3**, the reaction finished within 2 min using **4** as catalyst. The high reactivity of **4** permitted lowering the catalyst loading to a remarkable 0.05 mol% while maintaining a high yield of **2b** (1640 TON). Di-, tri-, and tetra-HDFs occurred for **1f–1h**, **1j**, and **1k** when higher amount of  $Et_2SiH_2$  (1.2–2.4 equiv.) were used. Several highly fluorinated phosphine compounds (**1i–1k**) utilized in various catalytic processes could be electronically fine-tuned through this HDF process.<sup>21</sup> Partially



**Figure 2.** (A) HDF of **1a**; <sup>19</sup>F NMR yields are given. (B) ORTEP drawings of **4** and **5**, with ellipsoids drawn at the 50% probability level. H atoms of **4** and **5**, the second molecule in the asymmetric unit of **4**, and disordered parts of **5** are omitted for clarity. Selected bond lengths (Å): for **4** (the bond lengths for the second molecule of **4** are given in brackets), Bi1–C1 2.189(3) [2.196(3)], Bi1–N1 2.525(3) [2.523(3)], Bi1–N2 2.503(3) [2.502(3)], N1–C2 1.288(4) [1.287(5)], N2–C3 1.288(4) [1.291(4)]; for **5**, Bi1–C1 2.201(2), Bi1–N1 2.5359(19), Bi1–N2 2.5142(18), N1–C2 1.282(3), N2–C3 1.284(3).

fluorinated substrates (**2a** and **1n**) and substrate with electron-neutral functionality (**1l**) were also amenable to HDF using **5** as catalyst. No directing effect was observed in HDF of **1m**, thus providing orthogonal selectivity to transition-metal-catalyzed systems.<sup>10f</sup> It should be mentioned that, similar to the reported systems based on transition metals, the HDF becomes sluggish when applied to polyfluoroarenes bearing electron-donating groups.<sup>9e,10d,i</sup> For instance, reaction of 2,3,4,5,6-pentafluorotoluene (**1o**) only delivered 2,3,5,6-tetrafluorotoluene (**2o**) in 3.5% yield after 3 days.

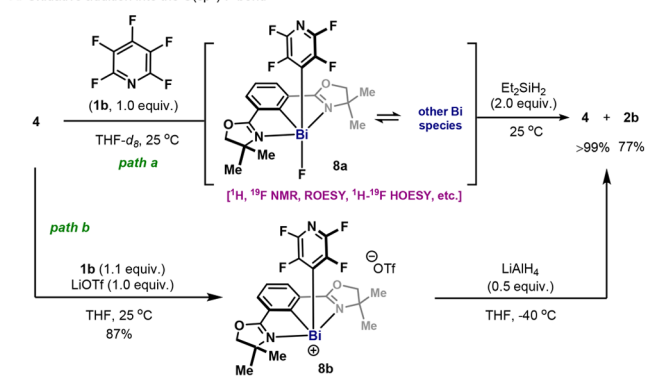
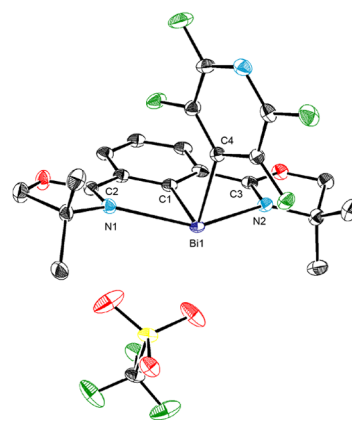
In light of its demonstrated high reactivity, **1b** was chosen as the model compound to study the mechanism of the Bi(I)-catalyzed HDF reaction. First, Phebox-Bi(I) (**4**) was subjected to 1.0 equiv. of **1b** in  $THF-d_8$  (Figure 3A, path a). After 5 min, <sup>19</sup>F NMR at 25 °C showed a distinct multiplet at –125.6 ppm, which is shifted dramatically compared to the *meta*-fluorines of **1b** and **2b** (**1b**, –163.0 ppm; **2b**, –141.7 ppm). However, such chemical shift is consistent with the *ortho*-fluorines of 4-tetrafluoropyridyl attached to Bi in the reported Bi(4-C<sub>5</sub>F<sub>4</sub>N)<sub>3</sub> (–120.7 ppm)<sup>22</sup> and to other electropositive centers (e.g., Mg,<sup>14f</sup> Ni<sup>23</sup>). <sup>1</sup>H–<sup>19</sup>F HOESY data at –40 °C further revealed the spatial proximity between these fluorines and two of the methyl groups of the Phebox backbone, suggesting the formation of Phebox-Bi(III)(4-tetrafluoropyridyl) fluoride (**8a**) via OA. However, the complex interconversions observed between **8a** and other Bi species precluded its complete characterization.<sup>18</sup> Nevertheless, when this mixture was treated with 2.0 equiv. of  $Et_2SiH_2$ , regeneration of **4** (>99%) and formation of the HDF product **2b** (77%) were observed,

Table 1. Scope of the Bi(I)-Catalyzed HDF<sup>a</sup>

<sup>a</sup>Reactions performed on 0.25 mmol scale of **1b-1n**. <sup>b</sup>Yields calculated by quantitative <sup>19</sup>F NMR using 4-fluorotoluene as internal standard. <sup>c</sup>0.20 mmol scale of **1k**.

manifesting the capacity of forging a C(sp<sup>2</sup>)-H bond through a Bi(I)/Bi(III) redox event.

It was reasoned that the reactivity of the fluoride after C-F cleavage played an important role in the observed equilibria. Hence, it was envisaged that fluoride abstraction after OA would lead to a well-defined cationic bismuth species with higher stability. Indeed, when the same reaction was performed in the presence of 1.0 equiv. of LiOTf, the triflate salt **8b** was isolated in 87% yield (Figure 3A, path b). The attachment of the 4-tetrafluoropyridyl group to the Bi center results in the <sup>19</sup>F signals of the *ortho*-fluorines appearing in a region (-121.4 ppm) similar to the observed shift of **8a**. Moreover, the observation of diastereotopic methyl groups and methylene protons in the oxazolines of **8b** by <sup>1</sup>H NMR (CH<sub>3</sub>, 1.60 and 1.27 ppm; CH<sub>2</sub>, 4.59 and 4.56 ppm) confirms that the symmetry through the plane of Phebox ligand has been broken in **8b**. The X-ray crystal structure of **8b** confirms the weak interaction between the cationic Bi center and the triflate anion, as shown by the large distance between the closest oxygens of triflate and the Bi center (2.974 Å, Σ<sub>cov</sub>(Bi-O) = 2.14 Å, <sup>24</sup> Figure 3B). In spite of the cationic nature of **8b**, the Bi1-C4 bond is still polarized [2.294(2) Å].<sup>25</sup> As a result, **8b** is highly moisture-sensitive, yielding [Phebox-Bi(OTf)]<sub>2</sub>O, **2b**, and other oxo-bismuth species upon hydrolysis.<sup>18</sup> Similar reactivity has been observed for Bi(4-C<sub>3</sub>F<sub>4</sub>N)<sub>3</sub><sup>22</sup> and other

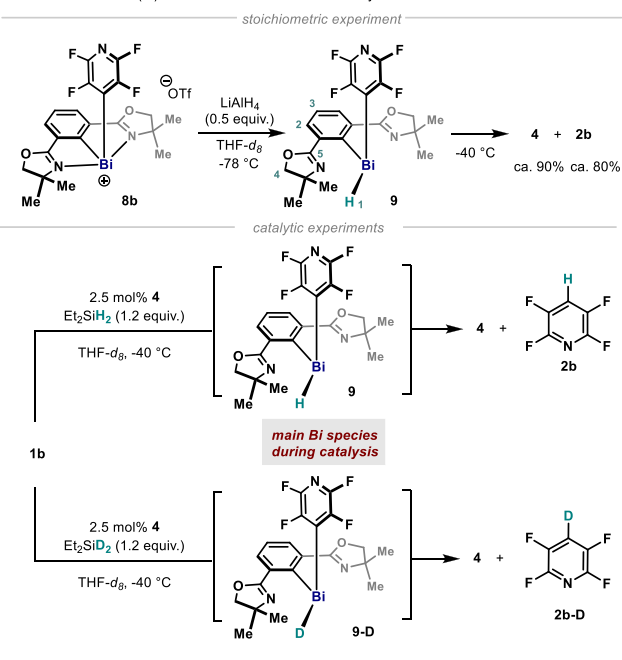
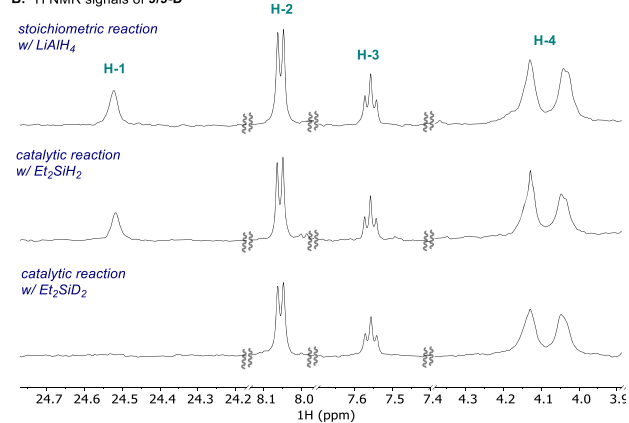
A. Oxidative addition into the C(sp<sup>2</sup>)-F bondB. XRD of **8b**

**Figure 3.** (A) OA of **4** with **1b**; path a: **4** (20.8 μmol) and **1b** (1.0 equiv.) in 0.5 mL of THF-*d*<sub>8</sub> at 25 °C; path b: **4** (2.08 mmol), **1b** (1.1 equiv.) and LiOTf (1.0 equiv.) in 7.0 mL of THF at 25 °C. (B) ORTEP drawing of **8b**, with ellipsoids drawn at the 50% probability level. H atoms of **8b** are omitted for clarity. Selected bond lengths (Å) and angles (°): Bi1-C1 2.225(2), Bi1-C4 2.294(2), Bi1-N1 2.450(2), Bi1-N2 2.4779(19), N1-C2 1.280(3), N2-C3 1.286(3); C1-Bi1-C4 93.60(8).

perfluoro-aryl<sup>26</sup> or -alkyl<sup>27</sup> Bi(III) compounds. Although **8b** showed no reactivity toward hydrosilanes due to the absence of fluoride anion, reduction of **8b** with stronger metal hydrides (e.g., LiAlH<sub>4</sub>) readily yielded **4** and **2b** (Figure 3A, path b).

At this point, it was hypothesized that a Ar<sub>2</sub>Bi(III)-H was generated via LM of **8a** or **8b** with hydrosilanes or metal hydrides. Organobismuth(III) hydrides are usually unstable species,<sup>28</sup> prone to H<sub>2</sub> release and formation of metallic Bi,<sup>29</sup> Bi(I),<sup>6a,16</sup> or dimetallic Bi(II)-Bi(II) compounds.<sup>7,30</sup> Reported by Power in 2000, (2,6-Mes<sub>2</sub>H<sub>3</sub>C<sub>6</sub>)<sub>2</sub>BiH represents the only stable and well-defined organobismuth hydride until now.<sup>31</sup> This compound indicated an alternative reaction pathway, namely C-H/D bond formation, yielding stable dibismuthene [Ar-Bi(I)=Bi(I)-Ar] and Ar-H/D (Ar = 2,6-Mes<sub>2</sub>H<sub>3</sub>C<sub>6</sub>). Later, the hydride signal of this bismuth position was located at a remarkably deshielded position (19.39 ppm),<sup>32</sup> which resulted from the spin-orbital heavy-atom effect on the light atom (SO-HALA effect).<sup>30,33-35</sup> Treatment of **8b** with 0.5 equiv. of LiAlH<sub>4</sub> at -78 °C resulted in instant formation of a new organobismuth species (Figure 4A, top). A broad singlet at 24.52 ppm in <sup>1</sup>H NMR was detected (Figure 4B, top), suggesting that this species corresponds to Phebox-Bi(III)(4-tetrafluoropyridyl) hydride (**9**) with an electronic environment around Bi-H similar to that of the reported (2,6-Mes<sub>2</sub>H<sub>3</sub>C<sub>6</sub>)<sub>2</sub>BiH. In addition, **9** has an asymmetric and

## A. Identification of Bi(III)-H: under stoichiometric and catalytic conditions

B.  $^1\text{H}$  NMR signals of 9/9-D

**Figure 4.** (A) Proposed Bi-H/D intermediates (9/9-D) and C-H/D reductive elimination. (B)  $^1\text{H}$  NMR spectra of 9/9-D at  $-40\text{ }^\circ\text{C}$ ; top:  $\text{LiAlH}_4$  reduction of **8b**; middle: catalytic HDF of **1b**; bottom: catalytic HDF of **1b** using  $\text{Et}_2\text{SiD}_2$ .

dynamic structure, as revealed by the considerably broadened NMR signals of the oxazolines (e.g., H-4, Figure 4B) and *ortho*-fluorines of the 4-tetrafluoropyridyl ( $-117.9\text{ ppm}$ ).<sup>18</sup> At  $-40\text{ }^\circ\text{C}$ , **9** rapidly decayed into Phebox-Bi(I) (**4**) and HDF product (**2b**) in ca. 90% and 80% yields, indicating C(sp<sup>2</sup>)-H RE at the Bi center. Under catalytic conditions, **9** was the major species and remained relatively stable in concentration (Figure 4A and 4B, middle). Structural information on **9** was gathered from 2D NMR data of the reaction mixture. Particularly, C-5 (157.8 ppm) of **9** is noticeably more shielded than those of **4**, **6**, and **8b** (**4**, 172.7 ppm; **6**, 181.9 ppm; **8b**, 182.3 ppm), but similar to that of the precursor Phebox-Br (**10**, 161.9 ppm). These electronic differences suggest that the oxazolines remain uncoordinated to the Bi center in **9**, permitting the Bi center to adopt a trigonal pyramidal geometry. To further interrogate the nature of the unusual downfield proton signal, the catalytic reaction was performed using  $\text{Et}_2\text{SiD}_2$ . While all the signals assigned to **9** could be observed, the signal at 24.52 ppm did not appear in  $^1\text{H}$  NMR,

suggesting the formation of corresponding bismuth deuteride 9-D (Figure 4A and 4B, bottom). As expected, decomposition of 9-D results in formation of **2b-D**. It is important to point out that this is a distinct example where NMR spectroscopic data supports the involvement of an organobismuth hydride in a catalytic process, resulting in the formation of a C-H bond.

Taking **1b** as an example, a Bi(I)/Bi(III) catalytic cycle can be proposed (Figure 5). Bismuthinidene **4** undergoes OA to

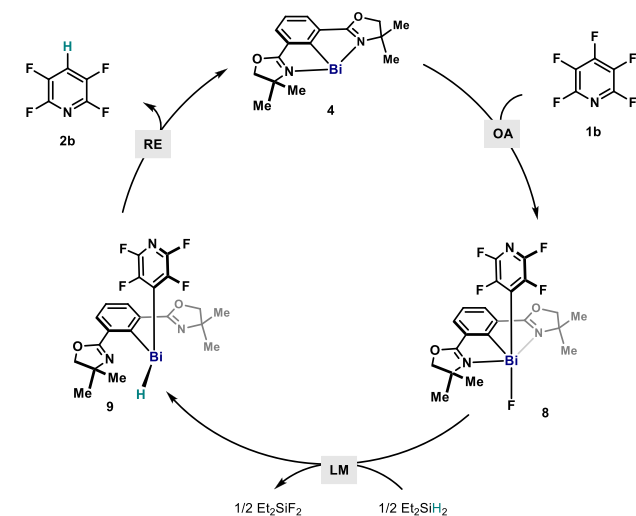


**Figure 5.** Proposed catalytic cycle for Bi(I)-catalyzed HDF.

**1b**, delivering the Bi(III) intermediate **8a**. Subsequent F/H LM between **8a** and  $\text{Et}_2\text{SiH}_2$  leads to the formation of diorganobismuth hydride (**9**) and fluorosilane. The catalytic redox loop is closed with RE from **9**, releasing HDF product (**2b**) and regenerating Bi(I) (**4**).

In conclusion, we present that bismuthinidenes supported by a Phebox ligand scaffold facilitate catalytic HDF reaction of a variety of polyfluoroarenes under mild conditions. Mechanistic investigations enabled the identification of the intermediates involved, both after C-F cleavage (**8b**) and prior to C-H bond formation (**9**). These findings support a distinct Bi(I)/Bi(III) redox cycle where Bi centers manifest oxidative addition, ligand metathesis, and reductive elimination steps, conventionally exploited in transition-metal catalysis. The facile cycling through three elementary organometallic steps in the Bi(I)/Bi(III) redox manifold serves as a response to the long-standing challenge in the field of redox catalysis using low-valent main-group compounds, potentially enabling a myriad of catalytic redox processes beyond HDF.

## ■ ASSOCIATED CONTENT

### Supporting Information

The Supporting Information is available free of charge at <https://pubs.acs.org/doi/10.1021/jacs.1c06735>.

Experimental procedures and analytical data ( $^1\text{H}$ ,  $^{13}\text{C}$ ,  $^{19}\text{F}$ , and  $^{31}\text{P}$  NMR, HRMS and X-ray crystallographic details) for new compounds (PDF)

### Accession Codes

CCDC 2091964–2091968 contain the supplementary crystallographic data for this paper. These data can be obtained free of charge via [www.ccdc.cam.ac.uk/data\\_request/cif](http://www.ccdc.cam.ac.uk/data_request/cif), or by emailing [data\\_request@ccdc.cam.ac.uk](mailto:data_request@ccdc.cam.ac.uk), or by contacting The

Cambridge Crystallographic Data Centre, 12 Union Road, Cambridge CB2 1EZ, UK; fax: +44 1223 336033.

## AUTHOR INFORMATION

### Corresponding Author

Josep Cornella – Max-Planck-Institut für Kohlenforschung, Mülheim an der Ruhr 45470, Germany; [orcid.org/0000-0003-4152-7098](https://orcid.org/0000-0003-4152-7098); Email: [cornella@kofo.mpg.de](mailto:cornella@kofo.mpg.de)

### Authors

Yue Pang – Max-Planck-Institut für Kohlenforschung, Mülheim an der Ruhr 45470, Germany; [orcid.org/0000-0002-5152-6876](https://orcid.org/0000-0002-5152-6876)

Markus Leutzsch – Max-Planck-Institut für Kohlenforschung, Mülheim an der Ruhr 45470, Germany; [orcid.org/0000-0001-8171-9399](https://orcid.org/0000-0001-8171-9399)

Nils Nöthling – Max-Planck-Institut für Kohlenforschung, Mülheim an der Ruhr 45470, Germany; [orcid.org/0000-0001-9709-8187](https://orcid.org/0000-0001-9709-8187)

Felix Katzenburg – Max-Planck-Institut für Kohlenforschung, Mülheim an der Ruhr 45470, Germany

Complete contact information is available at: <https://pubs.acs.org/10.1021/jacs.1c06735>

### Funding

Open access funded by Max Planck Society.

### Notes

The authors declare no competing financial interest.

## ACKNOWLEDGMENTS

Financial support for this work was provided by the Max-Planck-Gesellschaft, Max-Planck-Institut für Kohlenforschung and Fonds der Chemischen Industrie (FCI-VCI). Y.P. thanks CSC for a Ph.D. scholarship. This project has received funding from the European Union's Horizon 2020 research and innovation programme under Agreement No. 850496 (ERC Starting Grant, J.C.). We thank Prof. Dr. A. Fürstner for insightful discussions and generous support. We thank the MS, GC, and X-ray departments of Max-Planck-Institut für Kohlenforschung for analytical support. We thank Dr. R. Goddard for X-ray crystallographic analysis.

## REFERENCES

(1) (a) de Meijere, A.; Diederich, F. *Metal-Catalyzed Cross-Coupling Reactions*; Wiley-VCH Verlag GmbH & Co. KGaA: Mörtenbach, Germany, 2004; pp 1–64. (b) Crabtree, R. H. *The Organometallic Chemistry of the Transition Metals*; John Wiley & Sons: Hoboken, NJ, 2005; pp 163–184. (c) Hartwig, J. F. *Organotransition Metal Chemistry: From Bonding to Catalysis*; University Science Books: Mill Valley, CA, 2010; pp 877–965. (2) (a) Power, P. P. Main-Group Elements as Transition Metals. *Nature* **2010**, *463*, 171–177. (b) Chu, T.; Nikonov, G. I. Oxidative Addition and Reductive Elimination at Main-Group Element Centers. *Chem. Rev.* **2018**, *118*, 3608–3680. (c) Weetman, C.; Inoue, S. The Road Travelled: After Main-Group Elements as Transition Metals. *ChemCatChem* **2018**, *10*, 4213–4228. (d) Melen, R. L. Frontiers in Molecular p-Block Chemistry: From Structure to Reactivity. *Science* **2019**, *363*, 479–484. (e) Spikes, G. H.; Fettingner, J. C.; Power, P. P. Facile Activation of Dihydrogen by an Unsaturated Heavier Main Group Compound. *J. Am. Chem. Soc.* **2005**, *127*, 12232–12233. (f) Welch, G. C.; Juan, R. R. S.; Masuda, J. D.; Stephan, D. W. Reversible, Metal-Free Hydrogen Activation. *Science* **2006**, *314*, 1124–1126. (g) Frey, G. D.; Lavallo, V.; Donnadiou, B.; Schoeller, W. W.; Bertrand, G. Facile Splitting of Hydrogen and Ammonia by

Nucleophilic Activation at a Single Carbon Center. *Science* **2007**, *316*, 439–441. (h) Hicks, J.; Vasko, P.; Goicoechea, J. M.; Aldridge, S. Synthesis, Structure and Reaction Chemistry of a Nucleophilic Alumanyl Anion. *Nature* **2018**, *557*, 92–95. (i) Légaré, M.-A.; Bélanger-Chabot, G.; Dewhurst, R. D.; Welz, E.; Krummenacher, I.; Engels, B.; Braunschweig, H. Nitrogen Fixation and Reduction at Boron. *Science* **2018**, *359*, 896–900. (j) Rösch, B.; Gentner, T. X.; Langer, J.; Färber, C.; Eysel, J.; Zhao, L.; Ding, C.; Frenking, G.; Harder, S. Dinitrogen Complexation and Reduction at Low-valent Calcium. *Science* **2021**, *371*, 1125–1128.

(3) (a) Ruffell, K.; Ball, L. T. Organobismuth Redox Manifolds: Versatile Tools for Synthesis. *Trends in Chemistry* **2020**, *2*, 867–869. (b) Lipshultz, J. M.; Li, G.; Radosevich, A. T. Main Group Redox Catalysis of Organopnictogens: Vertical Periodic Trends and Emerging Opportunities in Group 15. *J. Am. Chem. Soc.* **2021**, *143*, 1699–1721.

(4) (a) O'Brien, C. J.; Tellez, J. L.; Nixon, Z. S.; Kang, L. J.; Carter, A. L.; Kunkel, S. R.; Przeworski, K. C.; Chass, G. A. Recycling the Waste: The Development of a Catalytic Wittig Reaction. *Angew. Chem., Int. Ed.* **2009**, *48*, 6836–6839. (b) van Kalker, H. A.; Leenders, S. H. A. M.; Hommersom, C. R. A.; Rutjes, F. P. J. T.; van Delft, F. L. In Situ Phosphine Oxide Reduction: A Catalytic Appel Reaction. *Chem. - Eur. J.* **2011**, *17*, 11290–11295. (c) Dunn, N. L.; Ha, M.; Radosevich, A. T. Main Group Redox Catalysis: Reversible P<sup>III</sup>/P<sup>V</sup> Redox Cycling at a Phosphorus Platform. *J. Am. Chem. Soc.* **2012**, *134*, 11330–11333. (d) van Kalker, H. A.; Bruins, J. J.; Rutjes, F. P. J. T.; van Delft, F. L. Organophosphorus-Catalyzed Staudinger Reduction. *Adv. Synth. Catal.* **2012**, *354*, 1417–1421. (e) Buonomo, J. A.; Aldrich, C. C. Mitsunobu Reactions Catalytic in Phosphine and a Fully Catalytic System. *Angew. Chem., Int. Ed.* **2015**, *54*, 13041–13044. (f) Zhao, W.; Yan, P. K.; Radosevich, A. T. A Phosphatene Catalyzes Deoxygenative Condensation of  $\alpha$ -Keto Esters and Carboxylic Acids via P<sup>III</sup>/P<sup>V</sup>=O Redox Cycling. *J. Am. Chem. Soc.* **2015**, *137*, 616–619. (g) Nykaza, T. V.; Cooper, J. C.; Li, G.; Mahieu, N.; Ramirez, A.; Luzung, M. R.; Radosevich, A. T. Intermolecular Reductive C–N Cross Coupling of Nitroarenes and Boronic Acids by P<sup>III</sup>/P<sup>V</sup>=O Catalysis. *J. Am. Chem. Soc.* **2018**, *140*, 15200–15205. (h) Longwitz, L.; Werner, T. Reduction of Activated Alkenes by P<sup>III</sup>/P<sup>V</sup> Redox Cycling Catalysis. *Angew. Chem., Int. Ed.* **2020**, *59*, 2760–2763.

(5) (a) Planas, O.; Wang, F.; Leutzsch, M.; Cornella, J. Fluorination of Arylboronic Esters Enabled by Bismuth Redox Catalysis. *Science* **2020**, *367*, 313–317. (b) Planas, O.; Peciukenas, V.; Cornella, J. Bismuth-Catalyzed Oxidative Coupling of Arylboronic Acids with Triflate and Nonaflate Salts. *J. Am. Chem. Soc.* **2020**, *142*, 11382–11387.

(6) (a) Wang, F.; Planas, O.; Cornella, J. Bi(I)-Catalyzed Transfer-Hydrogenation with Ammonia-Borane. *J. Am. Chem. Soc.* **2019**, *141*, 4235–4240. (b) Pang, Y.; Leutzsch, M.; Nothling, N.; Cornella, J. Catalytic Activation of N<sub>2</sub>O at a Low-Valent Bismuth Redox Platform. *J. Am. Chem. Soc.* **2020**, *142*, 19473–19479.

(7) (a) Schwamm, R. J.; Lein, M.; Coles, M. P.; Fitchett, C. M. Catalytic Oxidative Coupling Promoted by Bismuth TEMPO<sub>2</sub> Complexes. *Chem. Commun.* **2018**, *54*, 916–919. (b) Ramler, J.; Krummenacher, I.; Lichtenberg, C. Well-defined, Molecular Bismuth Compounds: Catalysts in Photochemically-induced Radical Decoupling Reactions. *Chem. - Eur. J.* **2020**, *26*, 14551–14555.

(8) (a) Kuehnel, M. F.; Lentz, D.; Braun, T. Synthesis of Fluorinated Building Blocks by Transition-Metal-Mediated Hydrodefluorination Reactions. *Angew. Chem., Int. Ed.* **2013**, *52*, 3328–3348. (b) Whitteley, M. K.; Peris, E. Catalytic Hydrodefluorination with Late Transition Metal Complexes. *ACS Catal.* **2014**, *4*, 3152–3159. (c) Hu, J.-Y.; Zhang, J.-L. Hydrodefluorination Reactions Catalyzed by Transition-Metal Complexes. In *Organometallic Fluorine Chemistry*; Braun, T., Hughes, R. P., Eds.; Springer International Publishing: Cham, 2015; pp 143–196.

(9) (a) Aizenberg, M.; Milstein, D. Catalytic Activation of Carbon-Fluorine Bonds by a Soluble Transition Metal Complex. *Science* **1994**, *265*, 359–361. (b) Vela, J.; Smith, J. M.; Yu, Y.; Ketterer, N. A.;

- Flaschenriem, C. J.; Lachicotte, R. J.; Holland, P. L. Synthesis and Reactivity of Low-Coordinate Iron(II) Fluoride Complexes and Their Use in the Catalytic Hydrodefluorination of Fluorocarbons. *J. Am. Chem. Soc.* **2005**, *127*, 7857–7870. (c) Reade, S. P.; Mahon, M. F.; Whittlesey, M. K. Catalytic Hydrodefluorination of Aromatic Fluorocarbons by Ruthenium *N*-Heterocyclic Carbene Complexes. *J. Am. Chem. Soc.* **2009**, *131*, 1847–1861. (d) Yow, S.; Gates, S. J.; White, A. J. P.; Crimmin, M. R. Zirconocene Dichloride Catalyzed Hydrodefluorination of C–F bonds. *Angew. Chem., Int. Ed.* **2012**, *51*, 12559–12563. (e) Lv, H.; Cai, Y.-B.; Zhang, J.-L. Copper-Catalyzed Hydrodefluorination of Fluoroarenes by Copper Hydride Intermediates. *Angew. Chem., Int. Ed.* **2013**, *52*, 3203–3207. (f) Cybulski, M. K.; McKay, D.; Macgregor, S. A.; Mahon, M. F.; Whittlesey, M. K. Room Temperature Regioselective Catalytic Hydrodefluorination of Fluoroarenes with *trans*-[Ru(NHC)<sub>4</sub>H<sub>2</sub>] through a Concerted Nucleophilic Ru–H Attack Pathway. *Angew. Chem., Int. Ed.* **2017**, *56*, 1515–1519.
- (10) (a) Braun, T.; Izundu, J.; Steffen, A.; Neumann, B.; Stammler, H.-G. Reactivity of a Palladium Fluoro Complex towards Silanes and Bu<sub>3</sub>SnCH=CH<sub>2</sub>: Catalytic Derivatisation of Pentafluoropyridine Based on Carbon–fluorine Bond Activation Reactions. *Dalton Trans.* **2006**, 5118–5123. (b) Breyer, D.; Braun, T.; Penner, A. Isolation and Reactivity of Palladium Hydrido Complexes: Intermediates in the Hydrodefluorination of Pentafluoropyridine. *Dalton Trans.* **2010**, 39, 7513–7520. (c) Fischer, P.; Götz, K.; Eichhorn, A.; Radius, U. Decisive Steps of the Hydrodefluorination of Fluoroaromatics using [Ni(NHC)<sub>2</sub>]. *Organometallics* **2012**, *31*, 1374–1383. (d) Lv, H.; Zhan, J.-H.; Cai, Y.-B.; Yu, Y.; Wang, B.; Zhang, J.-L.  $\pi$ - $\pi$  Interaction Assisted Hydrodefluorination of Perfluoroarenes by Gold Hydride: A Case of Synergistic Effect on C–F Bond Activation. *J. Am. Chem. Soc.* **2012**, *134*, 16216–16227. (e) Zhan, J.-H.; Lv, H.; Yu, Y.; Zhang, J.-L. Catalytic C–F Bond Activation of Perfluoroarenes by Tricoordinated Gold(I) Complexes. *Adv. Synth. Catal.* **2012**, *354*, 1529–1541. (f) Chen, Z.; He, C.-Y.; Yin, Z.; Chen, L.; He, Y.; Zhang, X. Palladium-catalyzed *Ortho*-selective C–F Activation of Polyfluoroarenes with Triethylsilane: A Facile Access to Partially Fluorinated Aromatics. *Angew. Chem., Int. Ed.* **2013**, *52*, 5813–5817. (g) Li, J.; Zheng, T.; Sun, H.; Li, X. Selectively Catalytic Hydrodefluorination of Perfluoroarenes by Co(PMe<sub>3</sub>)<sub>4</sub> with Sodium Formate as Reducing Agent and Mechanism Study. *Dalton Trans.* **2013**, 42, 13048–13053. (h) Gianetti, T. L.; Bergman, R. G.; Arnold, J. Carbon–fluorine Bond Cleavage in Fluoroarenes via a Niobium(III) Imido Complex: from Stoichiometric to Catalytic Hydrodefluorination. *Chem. Sci.* **2014**, *5*, 2517–2524. (i) Nakai, H.; Jeong, K.; Matsumoto, T.; Ogo, S. Catalytic C–F Bond Hydrogenolysis of Fluoroaromatics by [( $\eta^5$ -C<sub>3</sub>Me<sub>5</sub>)RhI(2,2′-bipyridine)]. *Organometallics* **2014**, *33*, 4349–4352.
- (11) (a) Senaweera, S. M.; Singh, A.; Weaver, J. D. Photocatalytic Hydrodefluorination: Facile Access to Partially Fluorinated Aromatics. *J. Am. Chem. Soc.* **2014**, *136*, 3002–3005. (b) Lu, J.; Khetrpal, N. S.; Johnson, J. A.; Zeng, X. C.; Zhang, J. “ $\pi$ -Hole- $\pi$ ” Interaction Promoted Photocatalytic Hydrodefluorination via Inner-Sphere Electron Transfer. *J. Am. Chem. Soc.* **2016**, *138*, 15805–15808.
- (12) Kikushima, K.; Grellier, M.; Ohashi, M.; Ogoshi, S. Transition-Metal-Free Catalytic Hydrodefluorination of Polyfluoroarenes by Concerted Nucleophilic Aromatic Substitution with a Hydrosilicate. *Angew. Chem., Int. Ed.* **2017**, *56*, 16191–16196.
- (13) Stahl, T.; Klare, H. F. T.; Oestreich, M. Main-Group Lewis Acids for C–F Bond Activation. *ACS Catal.* **2013**, *3*, 1578–1587.
- (14) (a) Jana, A.; Samuel, P. P.; Tavčar, G.; Roesky, H. W.; Schulzke, C. Selective Aromatic C–F and C–H Bond Activation with Silylenes of Different Coordinate Silicon. *J. Am. Chem. Soc.* **2010**, *132*, 10164–10170. (b) Samuel, P. P.; Singh, A. P.; Sarish, S. P.; Matussek, J.; Objartel, I.; Roesky, H. W.; Stalke, D. Oxidative Addition Versus Substitution Reactions of Group 14 Dialkylamino Metallylenes with Pentafluoropyridine. *Inorg. Chem.* **2013**, *52*, 1544–1549. (c) Chu, T.; Boyko, Y.; Korobkov, I.; Nikonov, G. I. Transition Metal-like Oxidative Addition of C–F and C–O Bonds to an Aluminum(I) Center. *Organometallics* **2015**, *34*, 5363–5365. (d) Crimmin, M. R.; Butler, M. J.; White, A. J. P. Oxidative Addition of Carbon–fluorine and Carbon–oxygen Bonds to Al(I). *Chem. Commun.* **2015**, *51*, 15994–15996. (e) Styra, S.; Melaimi, M.; Moore, C. E.; Rheingold, A. L.; Augenstein, T.; Breher, F.; Bertrand, G. Crystalline Cyclic (Alkyl)(amino)carbene-tetrafluoropyridyl Radical. *Chem. - Eur. J.* **2015**, *21*, 8441–8446. (f) Bakewell, C.; White, A. J. P.; Crimmin, M. R. Addition of Carbon–Fluorine Bonds to a Mg(I)–Mg(I) Bond: An Equivalent of Grignard Formation in Solution. *J. Am. Chem. Soc.* **2016**, *138*, 12763–12766. (g) Kysliak, O.; Görls, H.; Kretschmer, R. Cooperative Bond Activation by a Bimetallic Main-Group Complex. *J. Am. Chem. Soc.* **2021**, *143*, 142–148.
- (15) Lim, S.; Radosevich, A. T. Round-Trip Oxidative Addition, Ligand Metathesis, and Reductive Elimination in a P<sup>III</sup>/P<sup>V</sup> Synthetic Cycle. *J. Am. Chem. Soc.* **2020**, *142*, 16188–16193.
- (16) (a) Šimon, P.; de Proft, F.; Jambor, R.; Růžicka, A.; Dostál, L. Monomeric Organoantimony(I) and Organobismuth(I) Compounds Stabilized by an NCN Chelating Ligand: Syntheses and Structures. *Angew. Chem., Int. Ed.* **2010**, *49*, 5468–5471. (b) Vránová, I.; Alonso, M.; Lo, R.; Sedláč, R.; Jambor, R.; Růžicka, A.; Proft, F. D.; Hobza, P.; Dostál, L. From Dibismuthenes to Three- and Two-Coordinated Bismuthinidenes by Fine Ligand Tuning: Evidence for Aromatic BiC<sub>3</sub>N Rings through a Combined Experimental and Theoretical Study. *Chem. - Eur. J.* **2015**, *21*, 16917–16928.
- (17) (a) Denmark, S. E.; Stavenger, R. A.; Faucher, A.-M.; Edwards, J. P. Cyclopropanation with Diazomethane and Bis(oxazoline)-palladium(II) Complexes. *J. Org. Chem.* **1997**, *62*, 3375–3389. (b) Motoyama, Y.; Makihara, N.; Mikami, Y.; Aoki, K.; Nishiyama, H. Chiral Bis(oxazolonyl)phenyl Rhodium and Palladium Complexes. *Chem. Lett.* **1997**, *26*, 951–952. (c) Motoyama, Y.; Okano, M.; Narusawa, H.; Makihara, N.; Aoki, K.; Nishiyama, H. Bis(oxazolonyl)-phenylrhodium(III) Aqua Complexes: Synthesis, Structure, Enantioselective Allylation of Aldehydes, and Mechanistic Studies. *Organometallics* **2001**, *20*, 1580–1591. (d) Stol, M.; Snelders, D. J. M.; Godbole, M. D.; Havenith, R. W. A.; Haddleton, D.; Clarkson, G.; Lutz, M.; Spek, A. L.; van Klink, G. P. M.; van Koten, G. 2,6-Bis(oxazolonyl)phenylnickel(II) Bromide and 2,6-Bis(ketimine)-phenylnickel(II) Bromide: Synthesis, Structural Features, and Redox Properties. *Organometallics* **2007**, *26*, 3985–3994. (e) Bugarin, A.; Connell, B. T. Chiral Nickel(II) and Palladium(II) NCN-Pincer Complexes Based on Substituted Benzene: Synthesis, Structure, and Lewis Acidity. *Organometallics* **2008**, *27*, 4357–4369. (f) Bugarin, A.; Connell, B. T. A Highly Active and Selective Palladium Pincer Catalyst for the Formation of  $\alpha$ -Aryl Ketones via Cross-coupling. *Chem. Commun.* **2011**, 47, 7218–7220.
- (18) See Supporting Information for details.
- (19) These compounds have two independent molecules in the asymmetric units and the averaged bond distances are given in the text.
- (20) Wang, G.; Freeman, L. A.; Dickie, D. A.; Mokrai, R.; Benkő, Z.; Gilliard, R. J., Jr Isolation of Cyclic(Alkyl)(Amino) Carbene–Bismuthinidene Mediated by a Beryllium(0) Complex. *Chem. - Eur. J.* **2019**, *25*, 4335–4339.
- (21) (a) Ojima, I.; Kwon, H. B. Remarkable Effects of a Pentafluorophenyl Group on the Stereoselective Reactions of a Chiral Iron Acyl Complex. *J. Am. Chem. Soc.* **1988**, *110*, 5617–5621. (b) Hirai, T.; Hamasaki, A.; Nakamura, A.; Tokunaga, M. Enhancement of Reaction Efficiency by Functionalized Alcohols on Gold(I)-Catalyzed Intermolecular Hydroalkoxylation of Unactivated Olefins. *Org. Lett.* **2009**, *11*, 5510–5513. (c) Korenaga, T.; Abe, K.; Ko, A.; Maenishi, R.; Sakai, T. Ligand Electronic Effect on Reductive Elimination of Biphenyl from *cis*-[Pt(Ph)<sub>2</sub>(diphosphine)] Complexes Bearing Electron-Poor Diphosphine: Correlation Study between Experimental and Theoretical Results. *Organometallics* **2010**, *29*, 4025–4035. (d) Crisenza, G. E. M.; Sokolova, O. O.; Bower, J. F. Branch-Selective Alkene Hydroarylation by Cooperative Destabilization: Iridium-Catalyzed *ortho*-Alkylation of Acetanilides. *Angew. Chem., Int. Ed.* **2015**, *54*, 14866–14870. (e) Fernández, D. F.; Gulías, M.; Mascareñas, J. L.; López, F. Iridium(I)-Catalyzed Intramolecular Hydrocarbonation of Alkenes: Efficient Access to Cyclic Systems Bearing Quaternary Stereocenters. *Angew. Chem., Int.*

Ed. **2017**, *56*, 9541–9545. (f) Lee, Y. H.; Morandi, B. Palladium-Catalyzed Intermolecular Aryliodination of Internal Alkynes. *Angew. Chem., Int. Ed.* **2019**, *58*, 6444–6448.

(22) Tyrre, W.; Aboukacem, S.; Hoge, B.; Wiebe, W.; Pantenburg, I. Silver Compounds in Synthetic Chemistry: Part 4. 4-Tetrafluoropyridyl Silver(I), AgC<sub>5</sub>F<sub>4</sub>N in Redox Transmetalations—Possibilities and Limitations in Reactions with Group 15 Elements. *J. Fluorine Chem.* **2006**, *127*, 213–217.

(23) Schaub, T.; Fischer, P.; Steffen, A.; Braun, T.; Radius, U.; Mix, A. C–F Activation of Fluorinated Arenes using NHC-Stabilized Nickel(0) Complexes: Selectivity and Mechanistic Investigations. *J. Am. Chem. Soc.* **2008**, *130*, 9304–9317.

(24) Pyykkö, P.; Atsumi, M. Molecular Single-Bond Covalent Radii for Elements 1–118. *Chem. - Eur. J.* **2009**, *15*, 186–197.

(25) Hejda, M.; Jirásko, R.; Růžička, A.; Jambor, R.; Dostál, L. Probing the Limits of Oxidative Addition of C(sp<sup>3</sup>)–X Bonds toward Selected N,C,N-Chelated Bismuth(I) Compounds. *Organometallics* **2020**, *39*, 4320–4328.

(26) (a) Tyrre, W.; Naumann, D. On Pentavalent Perfluoroorgano Bismuth Compounds. *Can. J. Chem.* **1989**, *67*, 1949–1951. (b) Olaru, M.; Nema, M. G.; Soran, A.; Breunig, H. J.; Silvestru, C. Mixed Triorganobismuthines RAr<sub>2</sub>Bi [Ar = C<sub>6</sub>F<sub>5</sub>, 2,4,6-(C<sub>6</sub>F<sub>5</sub>)<sub>3</sub>C<sub>6</sub>H<sub>2</sub>] and Hypervalent Racemic Bi-chiral Diorganobismuth(III) Bromides RArBiBr (Ar = C<sub>6</sub>F<sub>5</sub>, Mes, Ph) with the Ligand R = 2-(Me<sub>2</sub>NCH<sub>2</sub>)C<sub>6</sub>H<sub>4</sub>. Influences of the Organic Substituent. *Dalton Trans.* **2016**, *45*, 9419–9428.

(27) Solyntjes, S.; Bader, J.; Neumann, B.; Stammler, H.-G.; Ignat'ev, N.; Hoge, B. Pentafluoroethyl Bismuth Compounds. *Chem. - Eur. J.* **2017**, *23*, 1557–1567.

(28) Aldridge, S.; Downs, A. J. Hydrides of the Main-Group Metals: New Variations on an Old Theme. *Chem. Rev.* **2001**, *101*, 3305–3366.

(29) Amberger, E. Hydride des Wismuts. *Chem. Ber.* **1961**, *94*, 1447–1452.

(30) Balázs, G.; Breunig, H. J.; Lork, E. Synthesis and Characterization of R<sub>2</sub>SbH, R<sub>2</sub>BiH, and R<sub>2</sub>Bi–BiR<sub>2</sub> [R = (Me<sub>3</sub>Si)<sub>2</sub>CH]. *Organometallics* **2002**, *21*, 2584–2586.

(31) Hardman, N. J.; Twamley, B.; Power, P. P. (2,6-Mes<sub>2</sub>H<sub>3</sub>C<sub>6</sub>)<sub>2</sub>BiH, a Stable, Molecular Hydride of a Main Group Element of the Sixth Period, and Its Conversion to the Dibismuthene (2,6-Mes<sub>2</sub>H<sub>3</sub>C<sub>6</sub>)BiBi(2,6-Mes<sub>2</sub>C<sub>6</sub>H<sub>3</sub>). *Angew. Chem., Int. Ed.* **2000**, *39*, 2771–2773.

(32) Olaru, M.; Duvinage, D.; Lork, E.; Mebs, S.; Beckmann, J. Heavy Carbene Analogues: Donor-Free Bismuthenium and Stibonium Ions. *Angew. Chem., Int. Ed.* **2018**, *57*, 10080–10084.

(33) Ashe, A. J.; Ludwig, E. G.; Oleksyszyn, J. Preparation and Properties of Dibismuthines. *Organometallics* **1983**, *2*, 1859–1866.

(34) Vicha, J.; Novotný, J.; Komorovsky, S.; Straka, M.; Kaupp, M.; Marek, R. Relativistic Heavy-Neighbor-Atom Effects on NMR Shifts: Concepts and Trends Across the Periodic Table. *Chem. Rev.* **2020**, *120*, 7065–7103.

(35) A few reports on the spectroscopic identification of organobismuth hydrides (R<sub>2</sub>BH) are known in the literature. Ashe (ref 33) and Breunig (ref 30) reported chemical shifts of 2.10–3.24 ppm for the hydrides of (alkyl)<sub>2</sub>BiH however, the hydride of Power's Ar<sub>2</sub>BiH appears at 19.39 ppm (ref 31). See ref 34 for more details.